LBNL-42252

CONF-9805106--

ERNEST ORLANDO LAWRENCE BERKELEY NATIONAL LABORATORY

New 3D Parallel SGILD Modeling and Inversion

Ganquan Xie, Jianhua Li,
and Ernest Majer

Earth Sciences Division

September 1998

Presented at the
18th Annual International Conference, "Predictability Quantifying Uncertainty in Models of Complex Phenomena,"
Los Alamos, NM,
May 11–15, 1998,
and to be published in
the Proceedings

DISCLAIMER

DISCLAIMER

LBNL-42252

New 3D Parallel SGILD Modeling and Inversion

Ganquan Xie, Jianhua Li, and Ernest Majer

Earth Sciences Division
Ernest Orlando Lawrence Berkeley National Laboratory
University of California
Berkeley, California 94720

September 1998

This work was supported partially by the Director, Office of Energy Research, Office of Basic Energy Sciences, of the U.S. Department of Energy under Contract No. DE-AC03-76SF00098.

LBNL-42252

NEW 3D PARALLEL SGILD MODELING and INVERSION

Ganquan Xie, Jianhua Li, and Ernest Majer

Earth Sciences Division

Lawrence Berkeley National Laboratory

September, 1998

This work was supported partially by the Office of Energy Research, Office of Basic Energy Sciences DOE under Contract No. DE-AC03-76SF00098.

New parallel SGILD modeling and inversion

Ganquan Xie, Jianhua Li, and Ernest Majer

Earth Sciences Division, Lawrence Berkeley National Laboratory

Abstract

In this paper, A new parallel modeling and inversion algorithm using a Stochastic Global Integral and Local Differential equation (SGILD) is presented. We derived new acoustic integral equations and differential equation for statistical moments of the parameters and field. The new statistical moments integral equation on the boundary and local differential equations in domain will be used together to obtain mean wave field and its moments in the modeling. The new moments global Jacobian volume integral equation and the local Jacobian differential equations in domain will be used together to update the mean parameters and their moments in the inversion. A new parallel multiple hierarchy substructure direct algorithm or direct-iteration hybrid algorithm will be used to solve the sparse matrices and one smaller full matrix from domain to the boundary, in parallel. The SGILD modeling and imaging algorithm has many advantages over the conventional imaging approaches. The SGILD algorithm can be used for the stochastic acoustic, electromagnetic, and flow modeling and inversion.

Key words: SGILD; modeling and imaging; stochastic; moments integral and differential equation

1 Introduction

Seismic, electromagnetic, and hydrology modeling and inversion are important for the prediction of oil, gas, coal, and geothermal energy reservoirs in geophysical exploration. Many imaging works in the geophysical research areas are used the determinstic frame. The deterministic inversion approaches are used to obtain the ensemble mean of the random target parameters. Because the data is incomplete and contaminated by noise, it is reasonable to study inverse and forward problem in the probability frame and to use stochastic approaches [1]. There are two ways to study the stochastic inversion, one is Markov chain Monte Carlo (MCMC) approach, other way is to recover the statistics moments of the parameters and fields using posterior probability optimization and annealing regularizing. Each approach has its own advantages and limitations.

In this paper, we developed a new parallel SGILD modeling and inversion using a stochastic global integral and local differential decomposition. The parameters and data are assumed to be random variables. We derived a new acoustic integral and differential equation system about the statistical moments of the mean, covariance, and standard deviation. A parallel SGILD algorithm is used to solve the moments integral and differential equations. The second order correction term can be used to improve the resolution of the mean impedance imaging. The parameter covariance and standard deviations can be used to estimate the uncertainty and construct a confidence interval for the acoustic velocity.

The new SGILD inversion method consists of five parts: (1) The domain is decomposed into subdomain SI and subdomain SII. (2) A new statistical moments global acoustic integral equation on the boundary and local differential equations in domain will be used together to obtain mean wave field and moment fields in the modeling step. (3) The new moments global Jacobian volume integral equation in SI and the local Jacobian differential equations in SII will be used together to update the mean velocity parameters and their moments from the random field data in the inversion step. (4) The subdomain SII can naturally be decomposed into 4^n smaller sub-cubic-domains; the sparse matrix in each sub-cubic- domain can be inverted separately, in parallel. (5) A new parallel multiple hierarchy substructure direct and direct-iteration hybrid algorithms will be used to solve the smaller full matrix in SI from domain to the boundary, recursively and in parallel.

The iteration of conventional nonlinear inversion includes two parts: (I) a finite element or finite difference scheme for differential equations with an absorption condition was used to obtain the seismic wave and EM field in the modeling step; (II) a discrete integral equation or its optimization was used to update the seismic velocity and electric conductivity in the inverse step. The limitations of the conventional nonlinear inversion are: (1) determinstic description of parameters will cause a disastrous ill posed inversion; (2) the inaccurate reflection error of the absorption boundary condition in part I enters the inversion domain as numerical noise, in particularly, the ill-posed property of the inversion will enhance the numerical noise that will cause divergence and low resolution; (3) the discrete integral equation in part II produces an ill-posed larger full matrix which is difficult or impossible to invert and to store; (4) the conjugate gradient (CG) iterations will become very slow due to the repeated calculation of the 3D Greens functions and the many complicated 3D integral terms. Moreover, since the ill-posed nonlinear optimization has many local minimum points, the CG iteration easily falls into a local minimum and gets a wrong or low resolution imaging.

The new SGILD parallel modeling and nonlinear inversion algorithm is designed to overcome the shortcomings of the conventional inversion. The advantages of the SGILD algorithm are: (1) Supposing the parameters and measured data are random variable, the new statistical moments acoustic and magnetic integral and differential equation will be together used to assess the posterior probability using Bayes theorem; (2) It uses new exact moments global boundary integral equations and local differential equations in the domain that reduces the numerical boundary noises and improves accuracy of the modeling and inversion; (3) Using a new moment global integral and local differential decomposition in inversion that decompose the ill-posed full matrix into 4^n small sparse matrices and a smaller full matrix, greatly improved the ill-posed condition, and reduced computation time and storage requirements; (4) The SGILD is a high performance parallel multiple hierarchy algorithm with parallel efficiency of 90 %; (5) it minimized data communication between processors that is suitable for the MPP T3E; (6) The moments of the parameters can be used to construct a confidence interval of the parameter. (7) the SGILD parallel algorithm can be widely useful to solve stochastic elliptic, parabolic, and hyperbolic modeling and inversion. The algorithm can be used for elastic wave, electromagnetic, and flow modeling and inversion, that will be a benefit for developing a new coupled GEO-HYDRO imaging. The new coupled stochastic modeling and high resolution imaging software will be useful for the prediction of oil, gas, coal, and geothermal energy reservoirs in geophysical exploration. This paper is constructed as follows: In section 1 we describe the stochastic acoustic equation and derive new moment Galerkin equations and boundary integral equations for forward modeling. The stochastic acoustic equations for nonlinear inversion are described in section 2, we derive the new moment volume integral equation and variation Garlerkin equations, translate the posterior probability optimization into a stochastic nonlinear regularizing optimization, and describe a Gauss-Newton annealing iteration. In section 4 we present the new parallel SGILD modeling and inversion algorithm using the global integral and local differential equations. Applications are described in section 5. Finally, we describe conclusions in section 6.

2 Stochastic acoustic equation for forward modeling

2.1 Stochastic differential equation

$$\frac{\partial}{\partial x}\left(\sigma\frac{\partial u}{\partial x}\right)+\frac{\partial}{\partial y}\left(\sigma\frac{\partial u}{\partial y}\right)+\frac{\partial}{\partial z}\left(\sigma\frac{\partial u}{\partial z}\right)+\omega^2 u=S\left(r,r_s\right) \tag{1}$$

where σ is the acoustic impedance, u is an acoustic wave function, ω is the angular frequency, S is a source term. Suppose that the σ is a random variable, the ω and S are deterministic variables, the acoustic wave, u, is a random variable. Substituting the perturbation expanding formula,

$$\begin{aligned} \sigma &= < \sigma > + \sigma_s, \\ u &= u_0 + u_1 + u_2 + \cdots, \end{aligned} \tag{2}$$

into (1), we have the following forward moment Galerkin equations

$$\int_{\partial\Omega_e} < \sigma > \frac{\partial u_0}{\partial n} \phi ds - \int_{\Omega_e} < \sigma > \nabla u_0 \nabla \phi d\Omega_e + \omega^2 \int_{\Omega_e} u_0 \phi d\Omega_e = \int_{\Omega_e} S \phi d\Omega_e, \tag{3}$$

and

$$\begin{aligned} FMG(< \sigma >, C_{u\sigma}, C_\sigma, u_0, \phi) = 0, \\ FMG(< \sigma >, C_u, C_{u\sigma}, u_0, \phi) = 0, \\ FMG\left(< \sigma >, < u_2 >, 1, \hat{C_{u\sigma}}, \phi\right) = 0, \end{aligned} \tag{4}$$

where

$$\begin{aligned} FMG(< \sigma >, C_{u\sigma}, C_\sigma, u_0, \phi) = \int_{\partial\Omega_e} < \sigma > \frac{\partial C_{u\sigma}(r', \Re)}{\partial n} \phi ds + \int_{\partial\Omega_e} C_\sigma \frac{\partial u_0}{\partial n} \phi ds \\ - \int_{\Omega_e} < \sigma > \nabla C_{u\sigma}(r', \Re) \nabla \phi d\Omega_e + \omega^2 \int_{\Omega_e} C_{u\sigma} \phi d\Omega_e - \int_{\Omega_e} C_\sigma \nabla u_0 \nabla \phi d\Omega_e, \end{aligned} \tag{5}$$

$< \sigma >$ is the mean of the acoustic impedance, $< u_0 >= u_0$, $< u_1 >= 0$, $< \sigma_s >= 0$, the head covariance $C_\sigma(r, \Re) =< \sigma_s(r)\sigma_s(\Re) >$, $C_u(r, \Re) =< u_1(r)u_1(\Re) >$, $C_{u\sigma}(r, \Re) =< u_1(r)\sigma_s(\Re) >$ is the cross covariance between the acoustic impedance and wave field, $\hat{C_{u\sigma}} = \{C_{u\sigma}\}_{\Re=r}$, ϕ is a basic testing function, Ω_e is a compact support set of the basic testing function ϕ.

2.2 Stochastic boundary integral equation

$$Au(r) = Bu_b(r) + \oint_{\partial\Omega_+} \sigma_b \frac{\partial G_b(r', r)}{\partial n} u(r) ds - \oint_{\partial\Omega_-} \sigma \frac{\partial u(r)}{\partial n} G_b(r', r) ds, \tag{6}$$

where $G_b(r', r)$ is background Green's function, $u_b(r)$ is incident wave, A and B are coefficients. Upon substituting (2) into (6), we have the following forward moment integral equations on the boundary:

$$Au_0(r) = Bu_b(r) + \oint_{\partial\Omega_+} \sigma_b \frac{\partial G_b(r',r)}{\partial n} u_0(r')\,ds - \oint_{\partial\Omega_-} <\sigma> \frac{\partial u_0(r')}{\partial n} G_b(r',r)\,ds, \qquad (7)$$

and

$$\begin{aligned} FMI\left(<\sigma>, C_{u\sigma}, C_\sigma, u_0, \phi\right) &= 0, \\ FMI\left(<\sigma>, C_u, C_{u\sigma}, u_0, \phi\right) &= 0, \\ FMI\left(<\sigma>, <u_2>, 1, \hat{C_{u\sigma}}, \phi\right) &= 0, \end{aligned} \qquad (8)$$

where

$$FMI\left(<\sigma>, C_{u\sigma}, \sigma_s^2, u_0, \phi\right) = AC_{u\sigma}(r',\Re) - \oint_{\partial\Omega_+} \sigma_b \frac{\partial G_b(r',r)}{\partial n} C_{u\sigma}(r',\Re)\,ds + \oint_{\partial\Omega_-} <\sigma> \frac{\partial C_{u\sigma}(r',\Re)}{\partial n} G_b(r',r)\,ds + \oint_{\partial\Omega_-} C_\sigma \frac{\partial u_0(r)}{\partial n} G_b(r',r)\,ds, \qquad (9)$$

We use the Galerkin finite element method to discretize the forward moment Galerkin equations (3) and (4), and the collocation finite element method to discretize the boundary integral equations (7) and (8),see [2] [4]. The discrete equations (3) and (7), (4) and (8) will be coupled as a complete equation system. The SGILD modeling algorithm will be used to solve the equations from the domain to the boundary, in parallel [3] [4].

3 Stochastic acoustic equations for nonlinear inversion

In this section, we describe the new stochastic acoustic volume integral equations and differential equations for nonlinear inversion.

3.1 Stochastic acoustic volume integral equation

$$u_d(r) = u_b(r) + \int_{V_s} (\sigma - \sigma_b) \nabla G_b(r,r) \nabla u(r)\,dr, \qquad (10)$$

Because the measured data u, and the acoustic impedance, σ, are assumed to be random variables, the equation (10) becomes a stochastic first type nonlinear integral equation. Using the perturbation method we have

$$\delta u_d(r) = \int_{V_s} \delta\sigma \nabla G_b\left(r,r\right) \nabla u\left(r\right) dr. \tag{11}$$

Substituting the expanding formulas,

$$\begin{gathered} \delta u_d(r) = < \delta u_d(r) > + \delta u_{d,s}(r), \\ u = < u > + u_s, \\ and \\ \delta\sigma = \delta\sigma_0 + \delta\sigma_1 + \delta\sigma_2 + \ldots.., \end{gathered} \tag{12}$$

into equation (11), we have the perturbation first type moments volume integral equations for inversion,

$$< \delta u_d(r) > = \int_{V_s} \delta\sigma_0 \nabla G_b\left(r,r\right) \nabla < u > \left(r\right) dr, \tag{13}$$

and

$$\begin{gathered} IMI(< u >, C_{\delta u_d}, C_{\delta\sigma u}, C_u, \delta\sigma_0) = 0, \\ IMI(< u >, C_{\delta\sigma\delta u_d}, C_{\delta\sigma}, C_{\delta\sigma u}, \delta\sigma_0) = 0, \\ IMI(< u >, 0, < \delta\sigma_2 >, 1, \hat{C_{\delta\sigma u}}) = 0, \end{gathered} \tag{14}$$

where

$$\begin{gathered} IMI(< u >, C_{\delta u_d}, C_{\delta\sigma u}, C_u, \delta\sigma_0) = C_{\delta u_d} \\ - \int_{V_s} C_{\delta\sigma u} \nabla G_b\left(r,r\right) \nabla < u > \left(r\right) dr + \int_{V_s} \delta\sigma_0 \nabla G_b\left(r,r\right) \nabla C_u\left(r\right) dr, \end{gathered} \tag{15}$$

IMI means the inverse moment integral equation, $< \sigma_1 >= 0$, $< u_s >= 0$, $C_{\delta u_d} =< \delta u_d(r)\delta u_d(\Re) >$, $C_{\delta\sigma u} =< \delta\sigma_1(r)\, u_s(\Re) >$, $C_u =< u_s(r)\, u_s(\Re) >$, $C_{\delta\sigma\delta u_d} =< \delta\sigma_1(r)\delta u_d(\Re) >$, $C_{\delta\sigma} =< \delta\sigma_1(r)\,\delta\sigma_1(\Re) >$, $\hat{C_{\delta\sigma u}} = \{C_{\delta\sigma u}\}_{\Re=r}$, they can be calculated in order of $C_{\delta\sigma u}$, $C_{\delta\sigma\delta u_d}$, and $C_{\delta\sigma}$.

3.2 A posterior probability optimization

Because equations (13) and (14) are ill posed, they can not be solved directly. We translate the inversion to the following posterior probability optimization problem,

$$P\left(\sigma|d\right) = \max. \tag{16}$$

Let

$$P(\sigma) = \frac{1}{\sqrt{2\pi}\hat{V}_\sigma} e^{-\frac{1}{2}\left(\frac{(-\Delta(\tilde{\sigma}-\bar{\sigma}),\tilde{\sigma}-\bar{\sigma})+(\tilde{\sigma}-\bar{\sigma})^2}{V_\sigma^2}\right)} \tag{17}$$

$$P(d|\sigma) = \frac{1}{\sqrt{2\pi}\hat{V}_{u_d}} e^{-\frac{1}{2}\frac{\|(u-u_d)\|^2}{V_{u_d}^2}} \tag{18}$$

By Bayes theorem,

$$P(\sigma|d) = \frac{P(d|\sigma)P(\sigma)}{\int P(d|\sigma)P(\sigma)\,dm}, \tag{19}$$

the optimization (16) is equvalent to the following stochastic nonlinear optimization of the random variable σ,

$$\frac{\|(u-u_d)\|^2}{V_{u_d}^2} + \left(\frac{(-\Delta(\tilde{\sigma}-\bar{\sigma}),\tilde{\sigma}-\bar{\sigma})+(\tilde{\sigma}-\bar{\sigma})^2}{V_\sigma^2}\right) = \min, \tag{20}$$

where $P(\sigma|d)$ is the posterior probability, $P(\sigma)$ is the prior probability on the acoustic velocity, $P(d|\sigma)$ is data probability based on the acoustic velocity model, Δ is the Laplacian operator, $\bar{\sigma}$ is the mean value of the random velocity that will be measured by core analysis or direct observation, $\tilde{\sigma}$ is the fitting distribution based on σ, u_d is the measured data with noises, V_{u_d} is the standard deviation of u_d, $\hat{V}_{u_d}$ is normalized deviation, V_σ is the standard deviation of σ, and $\hat{V}_\sigma$ is normalized deviation. Because there is incomplete information of V_σ which is measured in a few logging well or on the surface, we introduce a regularizing parameter α and translate (20) into the following stochastic nonlinear regularizing optimization,

$$\|(u-u_d)\|^2 + \alpha\left((-\Delta(\tilde{\sigma}-\bar{\sigma}),\tilde{\sigma}-\bar{\sigma})+(\tilde{\sigma}-\bar{\sigma})^2\right) = \min, \tag{21}$$

the regularizing parameter is relative to the confidence interval of the random velocity set.

3.3 Gauss-Newton iteration with annealing process

We use the modified annealing Gauss-Newton iterative method[5] to solve the optimization problem (21). The iteration scheme is as follows,

$$\left[\Im^T\Im - \alpha\Delta\right]\delta\sigma =$$

$$-\Im^T \left[u_d - u_b - \int\limits_{V_s} (\sigma - \sigma_b) \nabla G_b(r,r) \nabla u dr \right] + \alpha \Delta \sigma, \tag{22}$$

Upon substituting (12) into (22), we have

$$\begin{gathered} \left[\Im^T \Im - \alpha\Delta\right] \delta\sigma_0 = \\ \Im^T \left[< u_d > - u_b - \int\limits_{V_s} (< \sigma > - \sigma_b) \nabla G_b(r', r) \nabla < u > dr' \right] \\ -\alpha\Delta < \sigma >, \end{gathered} \tag{23}$$

$$\left[\Im^T \Im - \alpha\Delta\right] C_{\delta\sigma u} = \Im^T \left[C_{\delta u_d} - \int\limits_{V_s} \delta\sigma_0 \nabla G_b(r', r) \nabla C_u dr' \right] - \alpha\Delta C_{\sigma u},$$

$$\left[\Im^T \Im - \alpha\Delta\right] C_{\delta\sigma} = \Im^T \left[C_{\delta\sigma\delta u_d} - \int\limits_{V_s} \delta\sigma_0 \nabla G_b(r', r) \nabla C_{\delta\sigma u} dr' \right] - \alpha\Delta C_{\sigma},$$

$$\left[\Im^T \Im - \alpha\Delta\right] < \delta\sigma_2 > = -\Im^T \left[\int\limits_{V_s} \nabla G_b(r', r) \left(\nabla \hat{C}_{\delta\sigma u} \right) dr' \right], \tag{24}$$

where

$$\Im = \int\limits_{V_s} \nabla G_b(r', r) \nabla < u > \psi_e dr'. \tag{25}$$

After obtaining $< \delta\sigma_0 >, < \delta\sigma_2 >, C_{\delta\sigma u}$, and $C_{\delta\sigma}$, we can update $< \delta\sigma >, < \sigma >, C_{\sigma u}$, and C_σ using the follwing formula,

$$\begin{aligned} < \delta\sigma > &= < \delta\sigma_0 > + < \delta\sigma_2 >, \\ < \sigma >_{(n+1)} &= < \sigma >_{(n)} + \lambda < \delta\sigma >, \\ (C_{\sigma u})_{n+1} &= (C_{\sigma u})_n + \delta C_{\sigma u}, \\ (C_\sigma)_{n+1} &= (C_\sigma)_n + \delta C_\sigma. \end{aligned} \tag{26}$$

Substituting $< \sigma >$ and C_σ into (3) and (7), (4) and (8), we can calculate $< u_0 >$, $C_{u\sigma}$, C_u, u_2, and $< u >$. The circle is Gauss-Newton regularizing iteration. The parameter λ depends on the random annealing process [5] and the increment of δC_σ, The regularizing parameter is belong to $[0, \alpha_0]$ which depends on the standard deviation and covariance of the data and discrete error. The optimum regularizing parameter can be chosen by discrepancy principle [4] and [8], The ψ_e in (25) is a picewise constant base function.

3.4 Stochastic acoustic variation differential equation

The collocation finite element method is used to discretize the first type volume integral equation (23) and (24) and obtained full matrix equations. The high cost of computation time and storage is a serious limitation of the discrete integral equations of (23) and (24). A new parallel SGILD algorithm will be developed to overcoming this shortcoming in the next section.

Using SGILD algorithm, we don't need to solve the complete discrete volume integral equations on the whole domain, but only on a subdomain SI. In the subdomain SII, we solve the following moment Galerkin differential equations,

$$\begin{aligned}
&\int_{\partial\Omega_e} \delta\sigma_0 \frac{\partial < u >}{\partial n} \phi ds - \int_{\Omega_e} \delta\sigma_0 \nabla < u > \nabla\phi d\Omega_e \\
&\qquad = - \int_{\partial\Omega_e} < \sigma > \frac{\partial \delta < u >}{\partial n} \phi ds \\
&+ \int_{\Omega_e} < \sigma > \nabla\delta < u > \nabla\phi d\Omega_e - \omega^2 \int_{\Omega_e} \delta u \phi d\Omega_e,
\end{aligned} \tag{27}$$

and

$$\begin{aligned}
&IMG(< u >, \delta C_{\sigma u}, \delta C_u, C_u, C_{\sigma u}, \delta < u >, \delta\sigma_0, < \sigma >, \phi) = 0, \\
&IMG(< u >, \delta C_{\sigma}, \delta C_{\sigma u}, C_{\sigma}, C_{\sigma u}, \delta < u >, \delta\sigma_0, < \sigma >, \phi) = 0, \\
&\quad IMG\left(< u >, < \delta\sigma_2 >, 0, \hat{C}_{\delta\sigma u}, \hat{C}_{\sigma\delta u}, 1, 1, 0, \phi\right) = 0,
\end{aligned} \tag{28}$$

where

$$\begin{aligned}
&IMG(< u >, \delta C_{\sigma u}, \delta C_u, C_u, C_{\sigma u}, \delta < u >, \delta\sigma_0, < \sigma >, \phi) = \\
&\quad \int_{\partial\Omega_e} \delta C_{\sigma u} \frac{\partial < u >}{\partial n} \phi ds - \int_{\Omega_e} \delta C_{\sigma u} \nabla < u > \nabla\phi d\Omega \\
&\qquad + \int_{\partial\Omega_e} \delta\sigma_0 \frac{\partial C_u}{\partial n} \phi ds - \int_{\Omega_e} \delta\sigma_0 \nabla C_u \nabla\phi d\Omega \\
&\quad + \int_{\partial\Omega_e} < \sigma > \frac{\partial \delta C_u}{\partial n} \phi ds - \int_{\Omega_e} < \sigma > \nabla\delta C_u \nabla\phi d\Omega \\
&\quad + \int_{\partial\Omega_e} C_{\sigma u} \frac{\partial \delta < u >}{\partial n} \phi ds - \int_{\Omega_e} C_{\sigma u} \nabla\delta < u > \nabla\phi d\Omega,
\end{aligned} \tag{29}$$

Ω_e is a compact support set of the basic testing function ϕ, $\hat{C}_{\delta\sigma u} = \{C_{\delta\sigma u}\}_{\Re=r}$, $\hat{C}_{\sigma\delta u} = \{C_{\sigma\delta u}\}_{\Re=r}$. The moment Galerkin equations (27) and (28) are built on the subdomain SII. The Galerkin finite element method is used to discrete

(27) and (28) and to obtain the sparse matrix. The global volume integral equation (23) and local Galerkin equation (27) will be used to assemble a SGILD decomposition algorithm. Same SGILD algorithm is suitable for (24) and (28).

4 Parallel SGILD modeling and inversion algorithm

In the preceding sections, we have described two systems, integral equation system and differential equation system, for the stochastic acoustic modeling and inversion. A question is why do we need two systems for the modeling and inversion? A new parallel stochastic global integral and local differential decomposition algorithm, SGILD, for the modeling and inversion is presented in this section.

4.1 The conventional nonlinear inversion using the Gauss-Newton iteration

In the conventional nonlinear inversion using the Gauss-Newton iteration, the algorithm process is that (1) For giving coefficient parameter, using finite element or finite difference scheme to solve acoustic differential equation with an artificial absorption boundary condition to obtain the wave filed. (2) Solving a discrete norm equation of the regularizing optimization of the first type integral equation to update the velocity. (3) The step (1) and (2) constructed the Gauss-Newton iteration for the conventional nonlinear inversion. The regularizing Gauss-Newton nonlinear inversion is a robust approach, but the limitations are: (1) Along the iterations, the inaccurate reflection error of the absorption boundary condition in the forward modeling enters the inversion domain as numerical noise that will cause low resolution; (2) the discrete integral equation in the inversion produces an ill-posed larger full matrix which is difficult or impossible to invert and store. A new SGILD modeling and inversion algorithm is developed to overcome these limitations of the conventional nonlinear inversion.

4.2 New SGILD modeling and nonlinear inversion

For simplicity, we used a rectangular mesh for modeling and inversion. The unknown wave field and its moments are defined on the set of the nodes for modeling. The unknown velocity parameters and their moments are defined on the set of the cells for inversion. The new SGILD modeling and inversion method consists of three steps: First, in Figure 1, the domain is decomposed into a subdomain SI with white cells □ and a subdomain SII with dark cells ■ . This decomposition is called a cells-decomposition. The cells-decomposition should satisfy the following requirements: (1) the subdomain SI should include the boundary of the domain; (2) the subdomain SI should be a logical boundary of the subdomain SII; (3) the subdomain SII can be decomposed into $2^p \times 2^q \times 2^r$ subdomains for 3D problem or $2^p \times 2^q$ subdomains for 2D problem, the p, q, r are integer. The cells-decomposition induced a nodes-decomposition of the whole nodes of the domain, NSI and $NSII$. The subdomain NSI is the set of the boundary nodes ▪ and internal nodes •, i.e., the set of the nodes on the SI. The subdomain $NSII$ is the set of the internal circle nodes ∘ , i.e., the set of the inside nodes of SII. Second, suppose that the acoustic impedance mean $< \sigma >$ and the covariances are obtained by the previous iterative step, the discrete acoustic integral equation (7) and (8) on the boundary nodes and the discrete acoustic Galerkin differential equations (3) and (4) on the internal nodes of domain will be coupled to construct a complete equation system for the discrete moments of the acoustic wave field. The nodes-decomposition and multi-level parallel direct or direct-iteration hybrid methods can be used for solving the modeling equations. Third, after obtaining the wave field and its moments, the global discrete Jacobian volume integral equations (23-25) on cells of SI and the local discrete Jacobian differential equations (27-28) on cells of SII will be coupled to construct a complete equation system for updating the velocity. The cells-decomposition can be used for solving the equation system for updating parameters and their moments. The second step and third step are used to construct a loop of the parallel SGILD Gauss-Newton iteration. If the residual of the misfit between the model field moments and the measured field moments less than the giving tolerance then the iteration will be stop, otherwise the iteration should be running continuously. In the parallel program, the shared data, the shared do loops, and message passing interface (MPI) are used for communication and distribution of subdomain field data and matrix data on a massively parallel computer. In this parallel program, distribution of the jobs in the parallel processing is uniform and the parallel arrangement is done appropriately. The new global integral and local differential parallel inversion has been tested in the multiple processor of the Special Parallel Processing (SPP) in the CRAY-A.NERSC.GOV and the Massively Parallel computer T3D. The parallel effective rate is 80% to 96%. The detailed description of the new parallel SGILD modeling and inversion algorithm is presented in a Lawrence Berkeley National Laboratory technology reports [3] [4].

5 Applications

The SGILD algorithm can be used for the electromagnetic and flow modeling and inversion, see [6] and [7]. In [6], new magnetic boundary and volume integral equations for the moments of the resistivity, permittivity, and the magnetic field are derived[6] [7]. A 2.5D SGILD electromagnetic code is tested primarily using a synthetic and field data. The mean resistivity imaging and standard deviations are presented. In Figure 2, 16 frequencies, 6 electric line sources on the surface and 20 receivers in the vertical logging well are used to make synthetic data with Gaussian noise, the maximum standard deviation of the data is 5%. The high resolution imaging of the mean resistivity is obtained. The total maximum standard deviation (TSTD) of the resistivity is 11.8%, The local standard deviation (LSTD) of the resistivity of the target in left top corner (read) is 6%, The other local standard deviation of resistivity in right lower corner (blue) is 18.6%, that is because the read block is in the coverage area of the data site. The 2D mesh is 128x128, 64 x 30.5 CPU minites in T3E and 58 iterations are used to obtained these moments imaging. The optimization mean regularizing is $0.687456x10^{-6}$. Other resistivity imaging from practical field data in the geothermal exploration is presented in [6]. The field data configuration includes 16 frequencies, 6 electric line sources on the surface and 20 receivers in the vertical logging well. The maximum standard deviation of the field data is 21%. A reasonable mean resistivity imaging is obtained. The maximum standard deviation of the resistivity is 31.8%, The local standard deviation of resistivity near the borehole area is 19%, which is less than standard deviation of the field data. The second order mean term is effective to improve the resolution of the mean resistivity imaging. The 2D mesh is 256x256, optimization mean regularizing is $0.32934x10^{-1}$, the 64 x 3.8 CPU hours in T3E and 96 iterations were used to these moments imaging. The parallel rate of the primary SGILD code is 70% $\sim$ 90%. The SGILD acoustic velocity imaging and data configuration is presented in [6] and SGLID flow permeability inversion is presented in [7].

6 Conclusions

The primary tests shown that the SGILD modeling and inversion is a high resolution , robust stable, and high performance parallel imaging algorithm. There are obvious improvements of resolution of imaging from the field data. Actually, most of the conventional deterministic inversion approaches were only used to obtain the zero order mean of the target parameters, but no second order correction term and the standard deviation term. The SGILD algorithm can be used to obtain the improved ensemble mean parameter with second correction term, cross covarience between the parameter and field, and standard deviations of the parameters and field. These moments can be used to estimate the uncertainty and construct a confidence interval. The computational costs and storage of the stochastic modeling and inversion is $3 \sim 4$ times the deterministic inversion. The big cost can not be accepted in the workstation. The high performance SGILD algorithm overcomes the limitations. There are two ways to study the stochastic inversion, one is Markov chain Monte Carlo (MCMC) approach, other way is to recover the statistics moments of the parameters and fields using posterior probability optimization and annealing regularizing. Each approach has its own advantages and limitations. The moment equation approach to the single phase fluid forward modeling was presented by [9]. An advanced version of the SGILD algorithm will be developed to have the advantages both MCMC and MDE approaches.

References

[1] James Glimm, and David H. Sharp, Stochastic methods for the prediction of complex multiscale phenomena. *Report LAUR-97-3748, LANL,* (1997) 28.

[2] Ganquan Xie and Jianhua Li, A new algorithm for 3-D nonlinear electromagnetic inversion. 3-D Electromagnetic Method *SEG book P. 193-207. Editor: Oristaglio and Spies.*

[3] Ganquan Xie and Jianhua Li, A new 3D parallel high resolution electromagnetic nonlinear inversion based on global integral and local differential decomposition. *Report LBNL-40265, 1997.*

[4] Ganquan Xie, Jianhua Li, Ernest Majer, and D. Zou, New 3D parallel GILD electromagnetic modeling and nonlinear inversion using global integral and local differential equation. *Report LBNL-42105, 1998.*

[5] Ganquan Xie, Jianhua Li, and Ki Ha Lee, Annealing regularizing method for geophysical high resolution imaging. *Proceedings of the 3rd International SEG/Japan conference in Tokyo. 102-109, Nov. 8-10, 1995.*

[6] Ganquan Xie and Jianhua Li, New parallel SGILD stochastic seismic and EM modeling and inversion. *LBNL report, submitting to AGU annual meeting, 1998.*

[7] Ganquan Xie and Jianhua Li New parallel SGILD stochastic single phase flow modeling and inversion. *to be published in proceeding of Fourth IMACS International Symposium on Iterative Methods in Scientific Computation, 1998.*

[8] Ganquan Xie, Jianhua Li, and Y. M. Chen, Gauss-Newton-Regularizing method for solving coefficient inverse problem of PDE. *J. Comput. Math. vol. 5, no 1. 38-49, 1987.*

[9] Dongxiao Zhang and C. Larry Winter, Moment equation approach to single phase fluid flow in heterogeneous reservoirs *Submitted to SPEJ* (1997).

Funding

This work was supported partially by the Office of Energy Research and Office of Basic Energy Sciences of DOE under Contract NO. DE-AC0376SF00098.

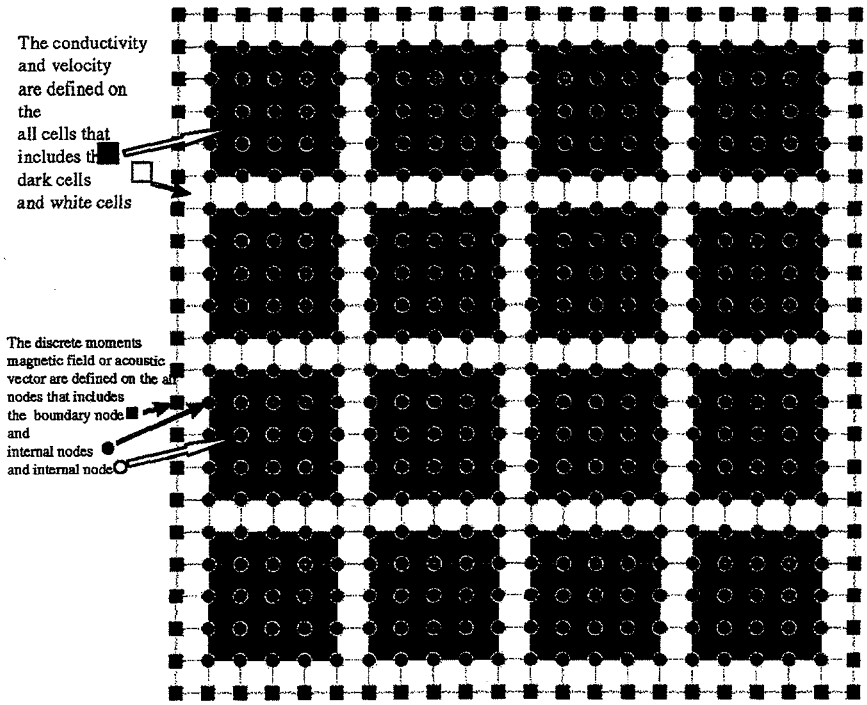

Figure 1. Domain decomposition for SGILD modeling and inversion

Parallel 2.5D SGILD mean resistivity imaging

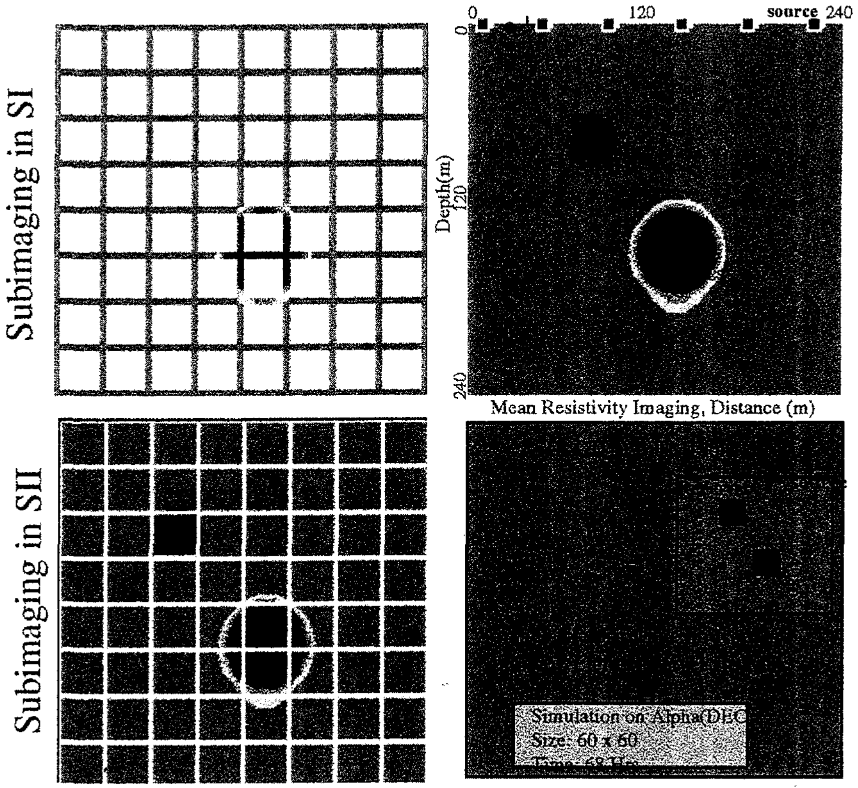

Figure 2. 2.5D electromagnetic SGILD resistivity imaging